Lawrence Berkeley Laboratory
UNIVERSITY OF CALIFORNIA

EARTH SCIENCES DIVISION

Presented at the 10th Annual Workshop on Geothermal
Reservoir Engineering, Stanford University,
Stanford, CA, January 22-24, 1985; and to be
published in the Proceedings

NUMERICAL STUDIES OF SILICA
PRECIPITATION/DISSOLUTION

C.H. Lai, G.S. Bodvarsson, and P.A. Witherspoon

January 1985

DO NOT MICROFILM
THIS PAGE

DISCLAIMER

This report was prepared as an account of work sponsored by an agency of the United States Government. Neither the United States Government nor any agency Thereof, nor any of their employees, makes any warranty, express or implied, or assumes any legal liability or responsibility for the accuracy, completeness, or usefulness of any information, apparatus, product, or process disclosed, or represents that its use would not infringe privately owned rights. Reference herein to any specific commercial product, process, or service by trade name, trademark, manufacturer, or otherwise does not necessarily constitute or imply its endorsement, recommendation, or favoring by the United States Government or any agency thereof. The views and opinions of authors expressed herein do not necessarily state or reflect those of the United States Government or any agency thereof.

DISCLAIMER

Portions of this document may be illegible in electronic image products. Images are produced from the best available original document.

NUMERICAL STUDIES OF SILICA PRECIPITATION/DISSOLUTION

C. H. Lai, G. S. Bodvarsson and P. A. Witherspoon

Earth Sciences Division
Lawrence Berkeley Laboratory
University of California
Berkeley, California 94720

INTRODUCTION

In hydrothermal systems, transport phenomena are complicated by coupled fluid, energy and chemical transport processes. Substantial quantities of energy and dissolved chemical species are carried by and also interact with the flow field; the potential field of energy and chemical species can also influence the flow field. These coupled processes often exhibit non-linear behavior, thus requiring numerical methods for solution. Many problems arise during the exploitation of geothermal systems that involve complicated transport processes.

One example is quartz precipitation near wells at the Cerro Prieto geothermal field, Mexico, caused by localized aquifer boiling (Truesdell et al., 1984). Boiling causes a gradual temperature decline and a consequent decrease in quartz solubility. Also separation of steam from the produced fluids can increase quartz concentrations in the residual water. Under such circumstances, quartz will precipitate after the concentration reaches a high degree of supersaturation, which results in reduction of permeability and mass flow rate.

Another example is silica scaling during reinjection operations. Reinjection is often employed in order to prevent chemical contamination of the environment by surface disposal and to enhance the energy recovery from the system. However, the spent brine often gets cooled below the saturation temperature so that deposition occurs in the surface pipelines, the disposal well or within the reservoir rock itself. If scaling occurs around the wellbore, permeabilities will be reduced and the injectivity of the well will decrease.

Keith et al. (1983) have conducted an experiment involving non-isothermal flow of supersaturated silica fluid through Westerly and Barre granite. Their experimental results confirm that silica precipitation by kinetic reactions with water is responsible for reductions in porosity, permeability and flow rate. Itoi et al. (1984) have performed an experimental study involving near-isothermal flow of geothermal fluid with supersaturated silica through a porous medium column. Their experimental results show that the silica scale is deposited mainly in the region near the fluid entry of the column, resulting in drastic permeability reduction.

APPROACH

Since the mechanisms of energy and chemical transport processes in subsurface geologic formations are too complicated to be described in detail, the convection-diffusion type equations are usually employed to model such transport processes. Over the last decade, many numerical schemes have been developed to solve such equations. However, it is difficult to construct finite difference methods which give accurate solutions. For example, it is well known that a higher-order difference method (Peaceman, 1977) may generate spurious oscillations or overshoot near the front for high Peclet numbers. A first-order upwind difference method will introduce numerical diffusion errors which may be several orders of magnitude larger than the effects of physical diffusion. To avoid these problems the method used in this study consists of a technique that utilizes monotonized upwind central differencing (Van Leer, 1977; Colella, 1984) and operator splitting (Strang, 1968).

In this paper we describe our numerical simulator PTC (pressure-temperature-chemistry), and also present the methods we use to reduce errors due to numerical diffusion. Examples of the application of this approach to two problems are included. The first problem involves non-isothermal flow of supersaturated silica through single fractures. The precipitation of silica in the fractures is modeled and the resulting permeability and flow rate decreases are calculated.

The second problem involves field data collected at the Ellidaar geothermal field in Iceland. After 15 years of fluid production, significant declines in pressure and temperature have been observed along with changes in silica concentrations. In order to illustrate the applicability of our model to such data, we have developed a simple numerical model that fits well with the observed production history. The applicability of our coupled method of analyzing the changing reservoir conditions is demonstrated, and the result is a more detailed understanding of the geothermal system.

NUMERICAL SIMULATOR PTC

The numerical simulator PTC was developed to analyze coupled hydrological-thermal-chemical processes encountered in subsurface geological formations. Development of the code PTC was based on the code PT (Bodvarsson, 1982), which handles coupled fluid and energy transport processes in porous/fractured media. In addition to fluid and energy transport processes, the code PTC can handle one-component chemical transport processes, including the effects of convection, dispersion, and kinetics of silica-water reactions. The transport equations used in the code PTC are briefly described below.

Governing Equations

The mass continuity equation can be expressed as:

$$\frac{\partial(\phi\rho_f)}{\partial t} + \nabla \cdot \bar{v}\,\rho_f = 0 \tag{1}$$

where $\bar{v}$ is Darcy's velocity expressed as:

$$\bar{v} = -\frac{k}{\mu}\left\{ \nabla p - \rho g \right\} \tag{2}$$

The equations for conservation of energy and chemical species in fractured/porous media can be expressed by Eqs. 3 and 4, respectively:

$$\frac{\partial[\phi\rho_f c_f T + (1-\phi)\rho_r c_r T]}{\partial t} + \nabla \cdot \rho_f c_f \bar{v} T$$

$$= \nabla \cdot K_h \nabla T + source \tag{3}$$

$$\frac{\partial(\phi\rho_f C)}{\partial t} + \nabla \cdot \rho_f \bar{v} C = \nabla \cdot \rho_f D\nabla C + source \tag{4}$$

Combining Eqs. 1 and 3 and linearizing the system properties, c_f, ρ_r, c_r, and ϕ, one obtains Eq. 5 for conservation of energy:

$$\sigma_T \frac{\partial T}{\partial t} + \rho_f c_f \bar{v} \cdot \nabla T = \nabla \cdot k_h \nabla T + source \tag{5}$$

where $\sigma_T = \phi\rho_f c_f + (1 - \phi)\rho_r c_r$

Similarly, the equation for conservation of chemical species can be expressed as:

$$\sigma_c \frac{\partial C}{\partial t} + \bar{v}\rho_f \cdot \nabla C = \nabla \cdot \rho_f D\nabla C + source \tag{6}$$

where $\sigma_c = \phi\rho_f$

SOLUTION TECHNIQUE

The method used to solve Eqs. 5 and 6 consists of a combination of the explicit monotonized upwind central difference method and the operator splitting technique. By means of operator splitting, the first fractional step is to remove diffusion and source terms from Eqs. 5 and 6. Thus, we solve the following equations:

$$\sigma_T \frac{\partial T}{\partial t} + \bar{v}_T \cdot \nabla T = 0 \tag{7}$$

and

$$\sigma_c \frac{\partial C}{\partial t} + \bar{v}_c \cdot \nabla C = 0 \tag{8}$$

where $\bar{v}_T = \bar{v}\rho_f c_f$ and $\bar{v}_c = \bar{v}\rho_f$

The method used to solve Eqs. 7 and 8 is the explicit monotonized central difference method proposed by Van Leer (1977) and developed for non-linear hyperbolic systems without operator splitting by Colella (1984). A detailed discussion of this method is given in Van Leer (1977) and Colella (1984). The second fractional step of operator splitting is to solve diffusion type equations such as Eqs. 9 and 10. These may be approximated by the implicit central difference method.

$$\sigma_T \frac{\partial T}{\partial t} = \nabla \cdot K_h \nabla T + source \tag{9}$$

$$\sigma_c \frac{\partial C}{\partial t} = \nabla \cdot \rho_f D\nabla C + source \tag{10}$$

Once Eqs. 7 and 8 have been solved, their solutions are used as initial conditions for Eqs. 9 and 10, which are solved for final temperature and concentration in a full step of operator splitting. A similar procedure allows one to move forward in time. At present, the code PTC implements this new numerical scheme for 1-D problems only; 2-D problems are solved with a conventional finite difference method.

VALIDATION OF NUMERICAL SCHEME

The validity of the numerical scheme has been tested against a simple problem for which an exact analytical solution is available. The test case considered is a one-dimensional iso-thermal chemical transport problem in a semi-infinite, isotropic porous medium. A constant concentration, C_0, is maintained at $x = 0$, and an initial concentration of zero is assumed. The fluid velocity (v/ϕ) and the longitudinal dispersion coefficient D_ℓ are assumed constant. The analytical solution to Eq. (8), for the given boundary and initial conditions, is given by Carslaw and Jaeger (1959) as:

$$\frac{C}{C_0} = \frac{1}{2}\left\{ erfc\left(\frac{x - \frac{vt}{\phi}}{2\sqrt{D_\ell t}}\right) + \exp\left(\frac{vx}{\phi D_\ell}\right) erfc\left(\frac{x + \frac{vt}{\phi}}{2\sqrt{D_\ell t}}\right)\right\}$$

$$\tag{11}$$

2

In the numerical calculations, the computational domain is divided into equal volume elements with a nodal point spacing of 0.5 m. The time step is kept below $\Delta x/(4\overline{V}_c\sigma_c)$ in order to obtain accurate results and avoid numerical instabilities. Calculations are made for a wide range of values for the Peclet number to thoroughly test the performance of the numerical scheme. The results are shown in Figure 1. The comparison between the numerical and analytical solutions shows excellent agreement for Peclet numbers less than 1. When the Peclet number is less than 100, the numerical diffusion errors are still small and there is no oscillation near the front. The numerical solution for a Peclet number of ∞ is very close to that for the Peclet number of 100.

It is of interest to compare the present numerical scheme to the conventional first-order upwind scheme. Figure 2 compares the two schemes for Peclet numbers 10 and 100. For problems with Peclet numbers below 2, the conventional central difference scheme can be employed to model the convection term with no oscillation results so that both schemes will show identical results. Figure 2 shows clearly that the conventional first-order upwind scheme will give large numerical diffusion errors, which are almost eliminated by the present scheme.

SILICA PRECIPITATION/DISSOLUTION MODEL

Capabilities for modeling silica precipitation and dissolution have also been developed. The silica equilibrium concentration is dependent on the temperature; the higher the temperature, the higher the silica equilibrium concentration. Thus, there is very strong coupling between the energy equation and silica reactions. In our numerical model, the approach proposed by Rimstidt (1980) for silica-water reactions is used. The rate equation for silica water reactions can be expressed as:

$$\frac{\partial C}{\partial t} = (\frac{A}{M_f}) \underline{K} (C_{eq} - C) \tag{12}$$

where (A/M_f) is the ratio of interfacial surface area of silica to the available fluid mass, $\underline{K}$ is the rate constant, and C_{eq} is the equilibrium concentration. For single fractures, the value of the reaction parameter A/M_f can easily be obtained from the fracture geometry as:

$$\frac{A}{M_f} = \frac{2}{b\rho_f} \tag{13}$$

where b is the fracture aperture and ρ_f is fluid density.

The permeability of a single fracture is assumed to be governed by the cubic law. By combining Eqs. (7) and (12), one can obtain a single component reactive silica transport equation for individual fractures. The numerical scheme described before is still valid;

the silica-water reaction term is considered as a source term in the second step of the splitting scheme.

APPLICATIONS

The numerical simulator is applied to two problems: (i) basic studies of reactive silica transport in fractures and (ii) exploitation modeling of the Ellidaar geothermal field, Iceland.

Reactive Silica Transport in a Single Fracture

The problem considered is that of a 50 m long fracture with an aperture of 10^{-4} m. Initially, the fracture contains 100°C fluid, with an equilibrium silica concentration of 142 ppm. In the numerical work, we use constant volume grid blocks, with a nodal point spacing of 0.5 m.

We first consider the isothermal problem of the injection of 100°C water supersaturated with 522 ppm of α-cristobalite. The results of numerical calculations are shown in Figures 3 through 5. Figure 3 shows the concentration and permeability distributions in the fracture. The concentration is represented by a dimensionless variable $[(C - C_{eq})/(C_b - C_{eq})]$, where C_b is the concentration of injection fluid and C_{eq} is the equilibrium concentration corresponding to the temperature of the injection fluid. The permeability is represented by a dimensionless ratio (k/k_i), where k_i is the initial permeability.

Figure 3 shows that the concentration front moves at a rate of approximately 0.3 m/day, with silica scaling occurring behind the front. The silica deposition causes reduction in the permeability, with the most severe reduction close to the inlet. We approximate the permeability changes from the aperture reduction and the cubic law (Witherspoon et al., 1980). The rate of silica deposition increases with time because the surface area to fluid mass factor (A/M_f) increases as the aperture decreases. This causes rapid permeability reduction close to the inlet at later times, and results in a small decrease in the concentration profile along the fracture.

Figure 4 shows a similar case, but with twice the initial flow rate. As expected, the speed of the concentration front is approximately double that of the first case, resulting in a much more rapid permeability decline close to the inlet.

Figure 5 shows the flow rate decline for both cases. The mass flow rate at the entrance is represented by a dimensionless variable Q/Q_i, where Q_i is the initial mass flow rate at the entrance. Figure 5 shows that the higher the initial flow rate at the inlet, the faster the dimensionless mass flow rate will decline because of greater silica precipitation. Qualitatively speaking, the effects of silica deposition on the transient flow behavior demonstrated by the numerical results are

similar to those observed in the experimental study of Itoi et al. (1984).

In order to investigate the coupling between mass and heat flow and silica transport processes, we next consider a problem with nonisothermal effects. For this case, the fracture fluids initially contain 150°C water with a silica concentration of 257 ppm (equilibrium value for β cristobalite) and 100°C water supersaturated with silica (522 ppm) enters the fracture at the inlet. Two cases are considered: (i) no heat losses to surroundings, and (ii) conductive heat transfer from the rock matrix to the fracture.

When heat transfer between the fracture fluids and the rock matrix is ignored, the results shown in Figure 6 are obtained. Dimensionless temperature is defined as $(T-T_i)/(T_b-T_i)$, where T_i is the initial fracture temperature (150°C) and T_b is the temperature of fluids at inlet (100°C). Figure 6 shows, as expected, that the velocities of the thermal and chemical fronts are identical (fracture porosity equals unity). The figure shows that behind the front the silica concentration is considerably higher at early time than the equilibrium concentration for 100°C water. This is because of the slow rate of reaction for silica-water at 100°C. Ahead of the thermal front, the silica concentration is in equilibrium with the 150°C water, and this causes a minimum in the silica concentration close to the location of the thermal and chemical fronts. The permeability at various times is similar to that obtained in the isothermal case (Figure 3).

When heat transfer between the fracture fluids and the surrounding rock matrix is considered, a different picture emerges, as shown in Figure 7. In this case the thermal front lags behind the chemical front, and because of the higher overall temperature, the silica deposition rate is much higher than in the previous case. This is reflected by the permeability profiles for the system at two different times. The plateau in the permeability profiles close to the inlet is due to the coupling between the temperature and the silica reaction rate. Although the deposition rate reaches a maximum value at different times depending on the distance from the inlet, eventually about the same cumulative amount of silica is deposited in the plateau region. Note that silica concentrations never go below the equilibrium value for 150°C.

FIELD EXAMPLE

One of the most important uses of numerical simulators for geothermal systems is to assess their generating capacity for power production or space heating. At present, the state of the art is to consider only the primary fluid component (water). If concentrations of dissolved solids or non-condensible gases are to be considered, one must modify the equation of state for the fluid. A major problem in geothermal reservoir assessment is the lack of

uniqueness of solutions to the nonlinear governing equations. We believe that multi-component modeling, i.e., including a method of handling the chemical variations that are observed, can yield solutions to geothermal problems that are more unique.

In this section we describe a simple model of the Ellidaar geothermal field, Iceland, where the temperature and pressure behavior in the reservoir as well as silica transients are investigated. All the data used in the analysis are taken from reports by Vatnaskil (1982, 1983). The conceptual model we use is shown in Figure 8. The reservoir consists of 110°C water with a silica concentration of about 150 ppm. During the 16-year exploitation of the field for space heating, considerable temperature decline has been observed and this has been associated with a decline in concentrations of silica in the produced fluids. One possible explanation of these transients is leakage of lower temperature fluids with less ppm silica from shallow aquifers. A connection of the reservoir with a shallow aquifer is shown on Figure 8. As the temperature gradient in the caprock is conductive it appears likely that the recharge from above is localized through fractures.

In simulating the conceptual model shown in Figure 8, we use the very simple numerical grid shown in Figure 9. It is a two layer radial grid with the whole well field lumped into a single element. Figure 10 shows the way in which the field has been exploited from 1968-81. Figures 11-13, show the way in which pressures, temperatures and silica concentrations respectively, have each declined with time. For simplicity, we assume a constant flow rate of 3.5×10^6 m³/year over the 16-year period, and neglect the seasonal and annual variations. Consequently, we do not attempt to model the effects of the seasonal variations shown on Figure 11.

Our primary purpose is not to develop a predictive model for the Ellidaar geothermal field, but rather to demonstrate the methodology and usefulness of multi-component modeling. After a brief trial and error process, we obtain the matches with the data shown in Figures 11-13. All of the matches appear reasonable considering the simple model assumed.

The main results of the history match are as follows. The match with the pressure decline data gives estimates of the permeabilities of the reservoir and the fractured caprock. We find that in order to match the temperature and the silica concentration decline (Figure 12), most of the fluid recharge to the reservoir must come from the shallow aquifer above. The main reservoir is quite permeable, but the rocks surrounding the wellfield are much less permeable (<5 md). The fractures providing cold water recharge from above also seem to be quite permeable. The best match with the pressure decline gave a rather high total compressibility, 4×10^{-7} pa^{-1}. This

4

high compressibility supports the idea of a
shallow unconfined aquifer hydrologically
connected to the main reservoir. The match
with the temperature decline gives an estimate
of the reservoir volume of approximately 2.5 x
10^8 m^3. Note that this is the reservoir
volume that has undergone cooling due to cold
water leakage from above. The average porosity
of the reservoir is determined by the match
with the silica decline (Figure 13). Our
results indicate an average porosity of 5%,
which appears reasonable for the volcanic rocks
present at Ellidaar.

Although we use a very simple conceptual
model in this study, our results nevertheless
illustrate that multi-component modeling can
give much information on reservoir properties
and characteristics. For example, this coupled
method enables us to obtain a good estimate of
reservoir volume as well as porosity, from
which reserve estimates can be made. As the
different processes are coupled, we believe
that the history match will be more unique and
consequently, future predictions more reliable.

SUMMARY AND CONCLUSIONS

(1)   A numerical scheme consisting of a monotonized,
      upwind central difference method and operator
      splitting technique has been developed for
      convection-diffusion type equations, which
      arise in energy and chemical transport
      processes. In contrast to conventional
      finite difference schemes the advantages
      of this numerical scheme are: (i) numerical
      diffusion errors are reduced significantly,
      and (ii) numerical results near sharp fronts
      are free of oscillations.

(2)   A model for simulating silica precipitation
      and dissolution has been developed. The
      model has been used for theoretical studies
      of silica deposition in single fractures.
      The results show that silica precipitation
      and the resulting permeability reduction
      depend strongly on the coupling between
      the chemical and thermal processes.
      Various examples are given for different
      flow rate declines and thermal effects.

(3)   The model has been applied to field data
      from the Ellidaar geothermal field in Iceland.
      A simple numerical grid was used for history
      matching with the declines of pressure,
      temperature, and silica concentration over
      a 16-year period. The results illustrate
      that multi-component modeling can yield
      detailed information about reservoir
      properties and characteristics.

ACKNOWLEDGEMENT

REFERENCES

Bodvarsson, G. S., Mathematical Modeling of the
    Behavior of Geothermal Systems under Exploita-
    tion, Ph.D. Dissertation, Lawrence Berkely
    Laboratory, LBL-13937, 1982, 353 pp.

Carslaw, H. S. and Jaeger, J. C., Conduction of
    Heat in Solids (2nd ed.), London, Oxford
    University Press, 1959, 510 pp.

Colella, P., Multidmensional upwind methods for
    hyperbolic conservation laws, J. Computa-
    tional Physics (to be published) 1984.

Itoi, R., MacKawa, H., Iukuda, M., Jinno, K.,
    and Hatanaka, K., Experimental study on
    the silica deposition in a porous medium,
    Geothermal Resources Council Transactions,
    Vol. 8, August 1984, pp. 301-304.

Keith, L. A., Delaney, P. T., and Moore, D. E.,
    Permeability reduction due to precipitation
    of quartz under nonisothermal conditions,
    Proc. Ninth Stanford Geothermal Workshop,
    December 13-15, 1983, pp. 239-245.

Peaceman, D. W., Fundamentals of Numerical
    Reservoir Simuation, Elsevier Scientific
    Publishing Company, Amsterdam-Oxford-New
    York, 1977.

Rimstidt, J. D., and Barnes, H. L., The
    kinetics of silica-water reactions,
    Geochim. Cosmochim, Acta, Vol. 44, 1980.

Strang, G., On the construction and comparison
    of difference schemes, SIAM J. Numer. Anal.,
    Vol. 5, September 1968, pp. 506-517.

Truesdell, A. H., D'Amore, F. and Nieva, D.,
    The effects of localized aquifer boiling on
    fluid production at Cerro Prieto, Geothermal
    Resources Council Transactions, Vol. 8,
    August 1984, pp. 223-229.

Van Leer, B., Towards the ultimate conservative
    difference scheme, J. Computational Physics,
    Vol. 23, 1977, pp. 276-299.

Vatnaskil, 1982, Ellidaar geothermal field -
    The effects of exploitation on the energy
    resources (report in Icelandic), prepared for
    the Reykjavik Municipal District Heating
    Systems, December, 1982.

Vatnaskil, 1983, Ellidaar geothermal field -
    Analysis of watertable and temperature
    measurements (report in Icelandic), prepared
    for the Reykjavik Municipal District Heating
    Systems, December, 1983.

Witherspoon, P,. A., Wang, J. S. Y., Iwai, K.
    and Gale, J. E., Validity of cubic law for
    fluid flow in a deformable rock fracture,
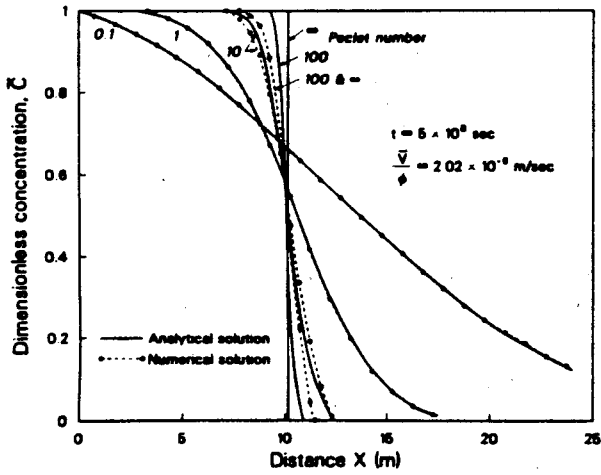   Water Resources Research, Vol. 16, No. 6,
    1980, pp. 1016-1024.

Fig. 1. Comparison between analytical and numerical solutions using the monotonized upwind central difference scheme for the convection-diffusion problem.
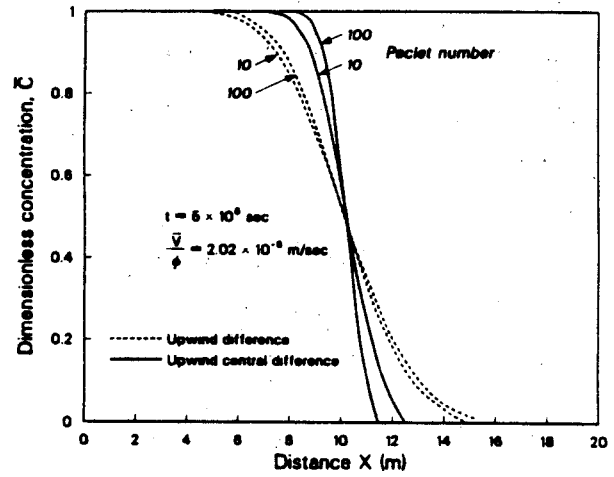

Fig. 2. Comparison between results using the monotonized upwind central difference scheme and using the first-order upwind difference scheme for the convection-diffusion problem.
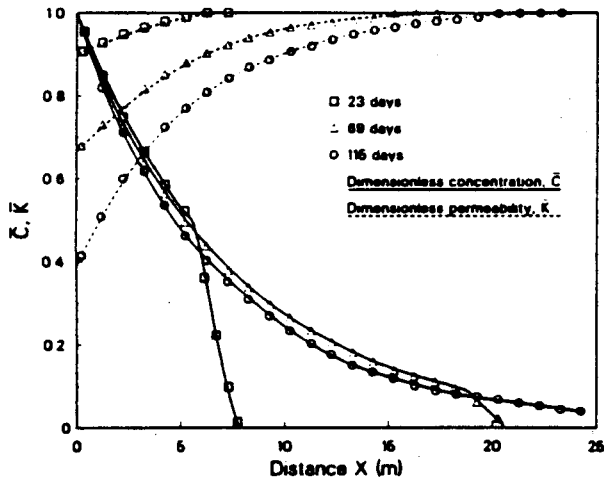

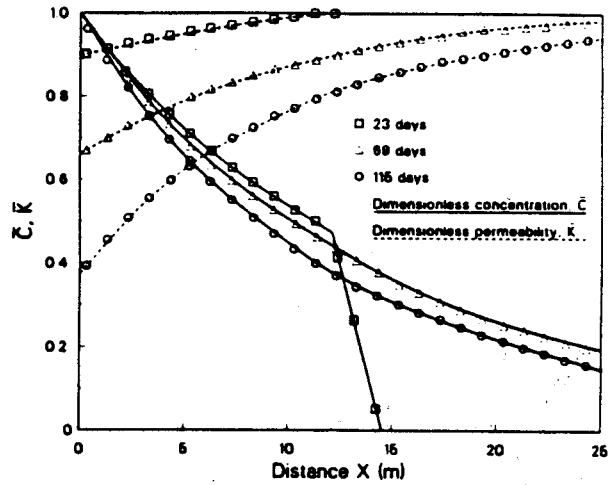Fig. 3. Silica concentration and permeability profiles along the fracture for the low pressure drop case.

Fig. 4. Silica concentration and permeability profiles along the fracture for the high pressure drop case.
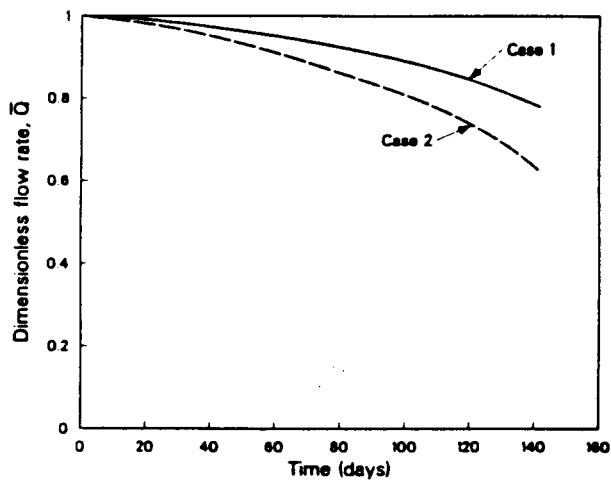
Fig. 5. Flow rate declines along the fracture under isothermal conditions for low pressure drop (Case 1) and high pressure drop (Case 2).
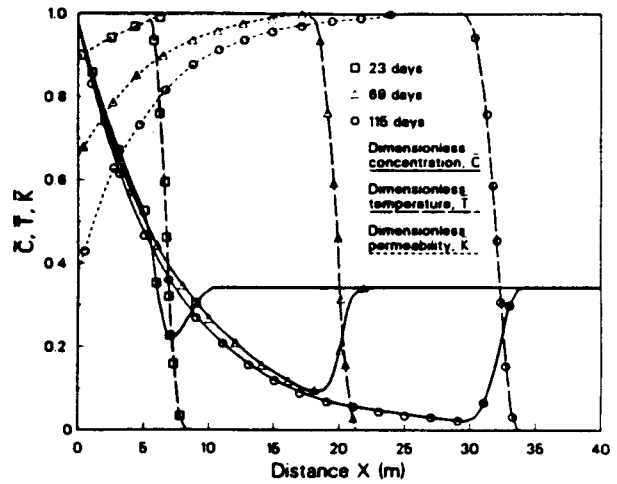
Fig. 6. Silica concentrations compared with temperature and permeability profiles along the fracture without heat transfer from the rock matrix.
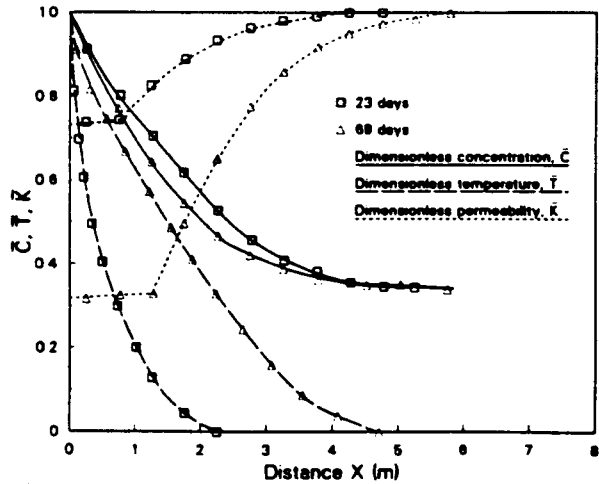
Fig. 7. Silica concentrations compared with temperature and permeability profiles along fractures with heat transfer from rock matrix.
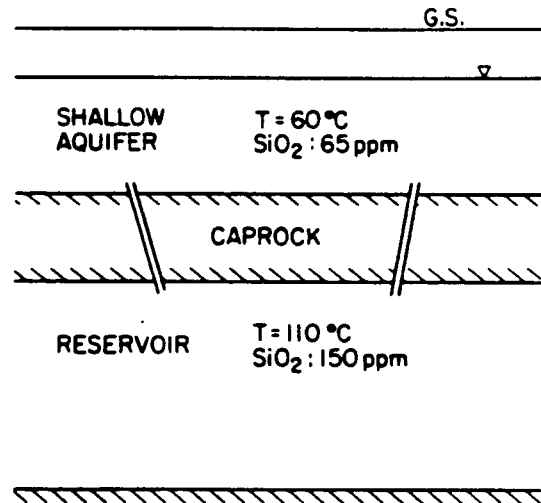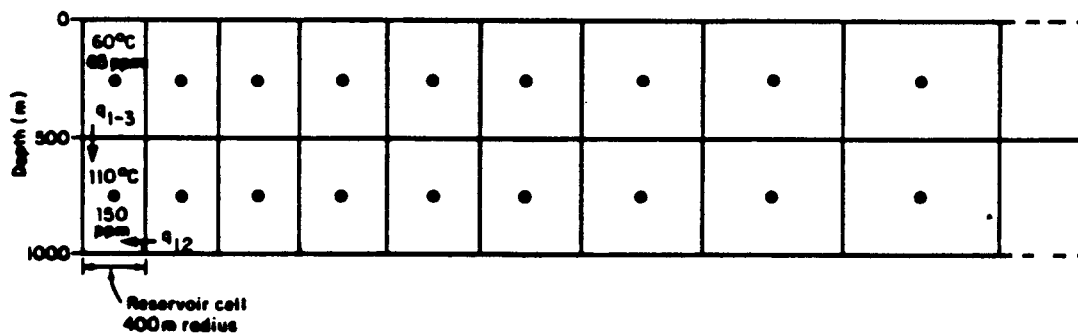

Fig. 8. A simplified conceptual model of the Ellidaar geothermal field, Iceland.

Fig. 9. The numerical grid used in the modeling the Ellidaar geothermal field.
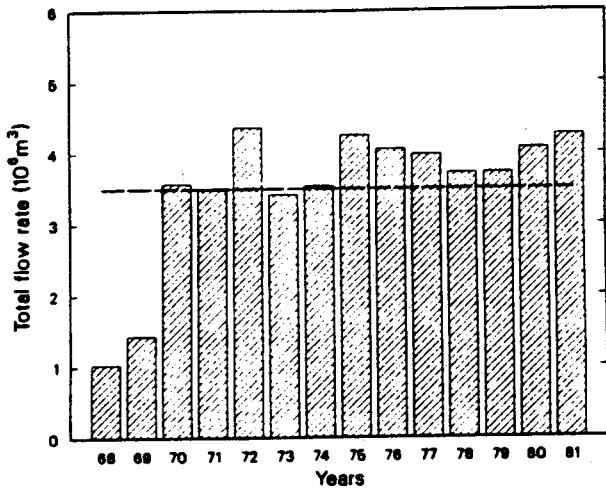
7

Fig. 10. Annual production rates for the
Ellidaar geothermal field. The
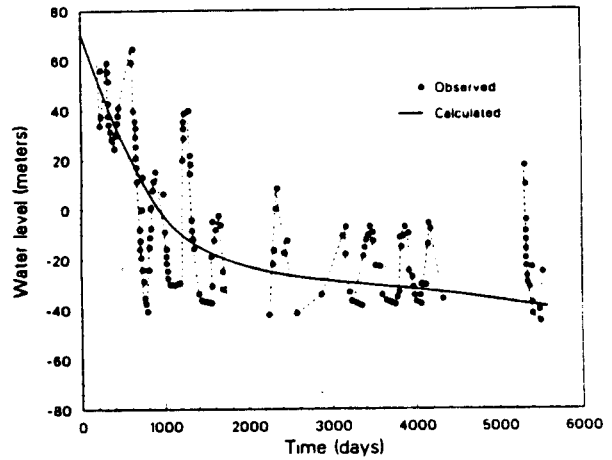broken line shows the average flow
rate used in the coupled modeling.

Fig. 11. Comparison betweeen calculated and
observed pressure decline at the
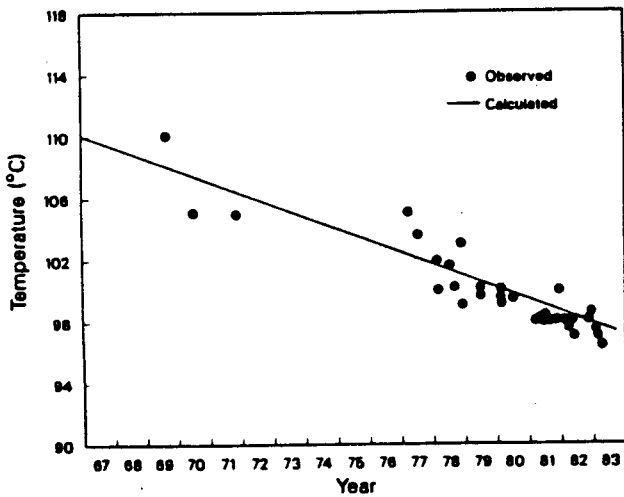Ellidaar field.

Fig. 12. Comparison between calculated and
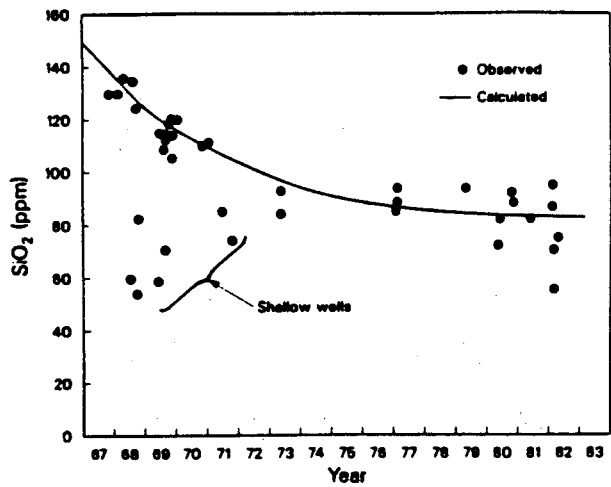observed temperature decline at
the Ellidaar field.

Fig. 13. Comparison between calculated and
observed silica concentration decline
at the Ellidaar field.